



Contents lists available at <http://qu.edu.iq>

## Al-Qadisiyah Journal for Engineering Sciences

Journal homepage: <http://qu.edu.iq/journaleng/index.php/IQES>



# Catalytic Oxidative Desulfurization of Heavy Naphtha Fraction Over a PMN550 Catalyst, Reactivity and a Kinetic Model

Najm Abed Hamdan <sup>a\*</sup>, Mohammed Ali Mutar <sup>b</sup>

<sup>a</sup> Chemical Engineering Dept., University of Al-Qadisiyah, Ad Diwaniyah, Iraq

<sup>b</sup> College of Sciences, University of Al-Qadisiyah, Ad Diwaniyah, Iraq

### ARTICLE INFO

#### Article history:

Received 6 August 2021

Received in revised form 6 September 2021

Accepted 8 September 2021

#### Keywords:

PMN550 catalysts

Catalytic oxidation of desulphurization (CODS)

Natural Zeolites

Brnsted acid sites

external and internal diffusion

### ABSTRACT

Desulfurization of heavy naphtha by a catalytic oxidation process combining hydrogen peroxide with organic and inorganic acids and in the presence of a PMN550 catalyst. This study was conducted to find out the effect of many variables on the efficiency of the process, especially the effect of hydrogen peroxide, the amount of acid, temperature, residence time, weight of the catalyst (0.01-0.6) g, temperature (20-120) C, residence time (20-140) minutes, ratio hydrogen peroxide to heavy naphtha (0.1-0.6) ml and ratio acid to heavy naphtha (0.01-0.175) ml. The catalytic oxidation process depends on all of the above variables. Desulphurization of heavy naphtha using organic and inorganic oxidizers in combination with hydrogen peroxide, glacial acetic acid, phthalic acid, malic acid, sulfuric acid and formic acid. The maximum removal of sulfur was with sulfuric acid and formic acid, which are 50%, 55%, respectively. The catalytic oxidation process carried out in two steps: the first step was the catalytic oxidation at a moderate temperature and atmospheric pressure, and the second step was to extract the oxidized mixture with a methanol-water mixture. The efficiency of the catalytic oxidation process carried out in the presence of PMN550 reached 99%. The catalyst was manufactured in the laboratory and a set of catalyst tests were performed on it FT-IR, AFM, BET, XRD, and XRF, which proven its efficacy. Mathematical models of the relevant reactions were developed to match the experimental results by obtaining the optimal kinetic parameters. Using optimization methods, the maximum conversion rate was 99%, at a temperature of 90°C, a residence time 60 minutes and the initial concentration was 651.3ppm.

© 2021 University of Al-Qadisiyah. All rights reserved.

## 1. Introduction

Sulfur oxides (SOX) are emitted to the atmosphere due to the combustion of fuel that is extracted from oil, and this emission constitutes a real threat to environmental deterioration and air quality pollution. It has been recommended all over the world to establish strict regulations regarding sulfur content in fuel to control these emissions [1,2] to avoid environmental degradation. The major partners, i.e. refiners and users, are

required to comply with these regulations for minimum or no sulfur emissions. This is possible if sweet petroleum fuels are manufactured in refining units before being supplied to consumers. The most widely used industrial method for removing sulfur compounds is Hydrous Desulfurization (HDS). This process has economic disadvantages due to the requirements of harsh process conditions such as high hydrogen

\* Corresponding author.

E-mail address: [Chem.post12@qu.edu.iq](mailto:Chem.post12@qu.edu.iq) (Najm Abed Hamdan)



pressure and high temperature for the catalytic decomposition of refractory organic sulfur compounds Yang [3]. Moreover, high activity (HDS) catalysts are in demand by the industry [4], therefore, searching for alternative operations that are low-cost and can operate in moderate conditions. Among these alternative processes to traditional HDS, bio desulphurization [6,7], desulphurization through adsorption Dasgupta et al. [5], electrochemical oxidation Wang et al. [9], ionic liquid extraction Li et al. [8] and oxidative desulphurization Trakarnpruk et al. [10]. Oxidation removal is gaining wide popularity in recent years as mentioned in the literature. due to its simple treatments and high efficiency. It consists of two steps: oxidation of organic sulfur compounds with appropriate oxidants, where these compounds are converted into sulfonates and sulfoxides.

The second step is to extract these sulfonates because of their relatively high polarity with some appropriate solvents. In the present work, some oxidants were investigated and compared. The oxidants used are hydrogen peroxide in combination with glacial acetic acid, phthalic acid, malic acid, sulfuric acid and formic acid. The catalytic oxidation of heavy naphtha (CODS) was carried out using air to aid the system. The present work, we carried out (CODS) of heavy naphtha using air assisted performic acid oxidation system in the presence of PMN550 catalysts. The reaction conditions (temperature, time and concentration of oxidants, i.e., H<sub>2</sub>O<sub>2</sub> and formic acid) were optimized.

## 2. Experimental

### 2.1. Materials

Formic acid (HCOOH) from (MACKLIN); Hydrogen Peroxide H<sub>2</sub>O<sub>2</sub> from (PanReacAppliChem); Acetic acid Glacial C<sub>2</sub>H<sub>4</sub>O<sub>2</sub> (Biosolve BV), Malic acid C<sub>4</sub>H<sub>6</sub>O<sub>5</sub> (BDH), Phthalic acid C<sub>8</sub>H<sub>6</sub>O<sub>4</sub> (MERCK), Sulfuric acid H<sub>2</sub>SO<sub>4</sub> (THOMMAS BAKER), Methanol CH<sub>3</sub>OH from (PubChem); Ethanol C<sub>2</sub>H<sub>5</sub>OH from (MERCK); Distilled water (Iraqi local product).

### 2.2. Heavy Naphtha

Experimental work was carried out on sample of Midland Refineries Company/ Daura refinery heavy naphtha. **Table 1** presents the physical characteristics of heavy naphtha.

**Table 1. Physical properties of heavy naphtha taken from Daura refinery**

Properties	
Spec. gravity at 15 Celsius	0.7377
Crude TBP cut points	100-170 Co
Expected ASTM Distillation D86	
Vol.%	Time
I.B. P	80 min
5%	92
10%	100
20%	106
30%	111
40%	116
50%	122
60%	127
70%	132
80%	138

90%	146
95%	154
E.B.P.	176
T.B. P	98
RES.	0.8
Sulfur content	651.3ppm
RON	40-50

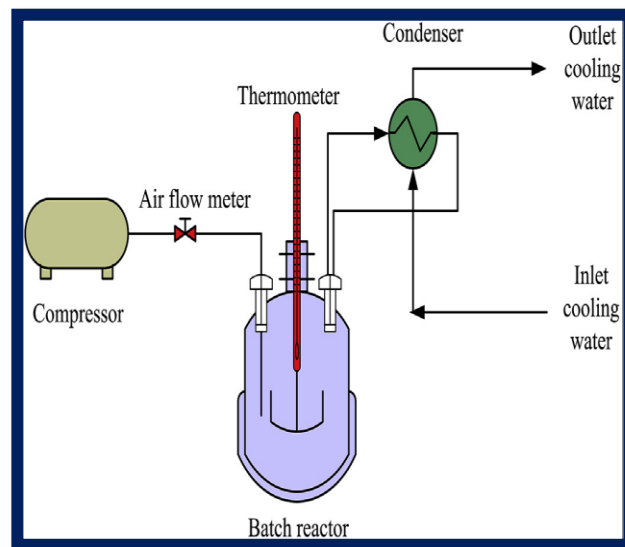


**Figure (1): Process diagram of batch reactor system.**

## 3. Preparation and Characterization of Catalyst (PMN550)

Natural zeolite is abundant in the Iraqi local markets, imported from many sources: India, Yemen, China and others. where the focus in this research is on the natural zeolite that is exported (India). After it has been prepared, developed and activated to be suitable for the catalytic oxidation process, for several reasons. First: its abundance, second: its low cost, and third: the nature of its composition. The natural Indian zeolite consists of Anorthite, Albite & Hematite rocks. As shown in the X-Ray Diffraction (XRD) examination. The method preparation, development and activation as a suitable catalyst for catalytic oxidation process (CODS). The raw natural zeolite was milled in the laboratory. The crushed natural zeolite was cross-linked by electric sieve shaker for 10 minutes. Then, it was dried overnight in an oven at 40°C, then (10g) natural zeolite, was calcined for (4 h) at 550°C. The powder was cooled to room temperature by turning off the furnace before the catalytic oxidation process. The synthesized catalysts were characterized by elemental analysis via XRD surface properties and XRF, FTIR, BET, TGA and AFM analysis.

## 4. Activity tests of the catalysts for ODS reactions

### 4.1.1. Batch reactor

The batch reactor has been utilized for carrying out sulfur compound reaction of oxidation. In addition, this reaction is carried out in a 500 mL flask with 3 necks and a round bottom. The middle neck is

linked to vertical condenser that condenses oil feedstock' vapors, allowing only air to get out. The other neck has been utilized as air inlet that's connected to compressor and the air is going to reach the flask bottom via glass tube, whereas the 3rd neck has been utilized for measuring flask temperature through the insertion of a thermometer into solution inside the flask and for withdrawing sample reaction in the case when the time has approached. The batch reactor is heated and mixed with the help of a heating mantle stirrer. The process diagram as well as the experimental device of ODS are shown in the two Figs (1) and (2).



Figure (3): Experimental device of CODS reactions

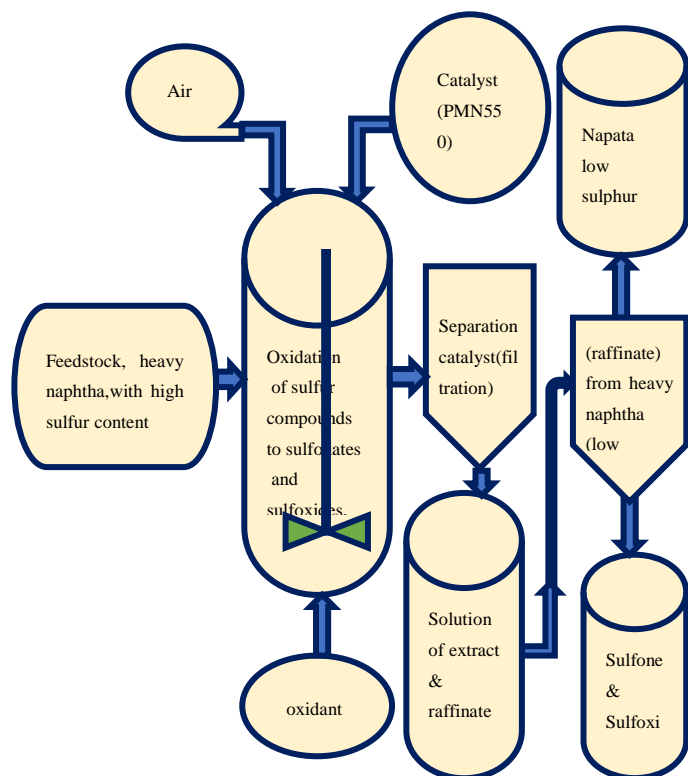


Figure (2): Schematic representation of the ODS system

#### 4.1.2. Catalytic oxidation of desulfurization (CODS) of Heavy Naphtha

Heavy naphtha ODS experiments were carried out using 20 mL of model oil in a 3-neck flask that has a condenser, which was placed in an oil bath that is mounted on a magnetic stirring hot plate. The sample was treated with 2.5ml formic acid, 2 ml H<sub>2</sub>O<sub>2</sub>, and 0.2g PMN550 catalyst. Utilizing Pyrex glass air bubbler, dry air has been bubbled through the reaction mix at a 150 ml/min flow rate and stirred for (20,40,60,80,100,120,140) min. with constant air bubbling and temperature maintained at (20,30,50,70,80,90,120)°C. Following oxidation, the sample has been mixed with an equal extraction solution volume (20:80 methanol/distilled water) and transferred into separating funnel, where oil layer has been separated. To achieve maximum sulfur removal, the temperature of the reaction and the time have been enhanced. The reactivity regarding various sulfur compounds has been studied via conducting reactions at various temperatures and withdrawing small aliquots from reaction sump at various times. The kinetics of oxidation were also investigated. Hydrogen peroxide and performic acid concentrations were optimized. It was also looked into the impact of extraction number on total desulfurization yields.



Figure (4): Extraction process for different operating conditions

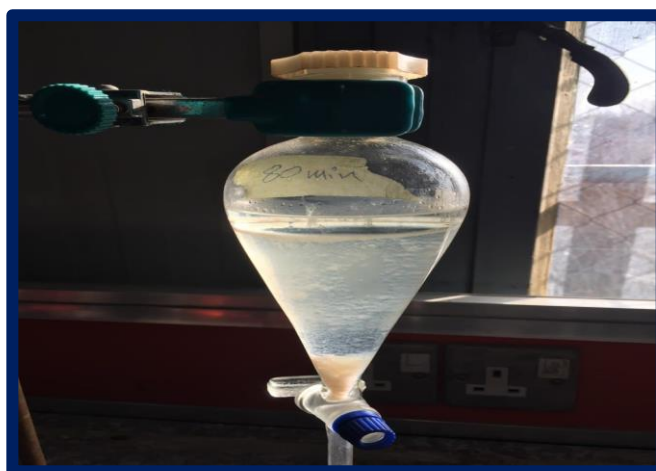


**Figure (5): Product of catalytic oxidation of sulfur compounds in naphtha**



**Figure(6): Catalytic oxidation product for different conditions**



**Figure(7): Changing the color of raffinate due to changing operational conditions and the amount of sulfur content also varies**

#### 4.1.3. Measurement of Sulfur concentration by ASTM D7039

The sulfur concentration has been determined through SINDIE OTG sulfur analyzer using the ASTM D7039 method. The SINDIE device provides enhanced accuracy and precision when measuring ultralow sulfur diesel and gasoline, as well as crudes and heavy fuel oil, because ASTM D7039 approach is optimum for refining industries, in which performance, reliability and detection are crucial. The device is located at the Ministry of Oil's Researches and Development Oil Centre.

#### 4.1.4. Total Sulfur Analyses

The total sulfur concentration in the samples has been determined using SN analyzer (Antek by PAL) with chemi-luminescence and a vacuum ultraviolet detector. As a carrier gas, argon was used, and pure oxygen was used as an oxidant. Analyses have been carried out in triplicates, with the average result indicated for every  $\mu\text{l}$  of injected samples. Using the next relation, the desulfurization yield related to the model oil has been calculated as % desulfurization.:

$$\% \text{Desulfurization} = \frac{S_o - S_t}{S_o} \times 100 \quad (1)$$

where the  $S_o$  represents the sulfur concentration of the original heavy naphtha and  $S_t$  represents the treated oil's sulfur concentration.

## 5. RESULTS AND DISCUSSION

### 5.1. Characterizations of the catalysts

The characterization of composite supports and the prepared catalysts provides information regarding morphology, structure, and the chemical composition. The information is vital to explain the relations between their physiochemical and chemical properties as well as on the catalytic activity.

### 5.2. Fourier transform infrared (FTIR) -Spectrum

FTIR spectra, illustrates that sharp feature appearing corresponded to hydroxyl groups of our PMN550 peak at  $3400 \text{ cm}^{-1}$  might be identified [28]. Also, the peak at the value of  $1183 \text{ cm}^{-1}$  is representing Si-O-Al and Si-O-Si bonds in a stretching mode. In addition,  $\text{TiO}_2$  showed strong absorption peaks at  $1402$  &  $1654 \text{ cm}^{-1}$ , FTIR bands at  $780 \text{ cm}^{-1}$  and  $1100 \text{ cm}^{-1}$  might be allocated to asymmetric and symmetric stretching vibration values of Si-O-Si linkage regarding the model of the zeolite [29][30]. The vibration modes of  $1046 \text{ cm}^{-1}$  and  $793 \text{ cm}^{-1}$  have been assigned to internal vibration of  $\text{SiO}_4$ . The H-OH bending vibrations related to molecules of water that were adsorbed have been identified at  $1625 \text{ cm}^{-1}$ . FTIR spectroscopy thoroughly detects the acidic groups of the hydroxyl OH of solid catalysts [12][13].

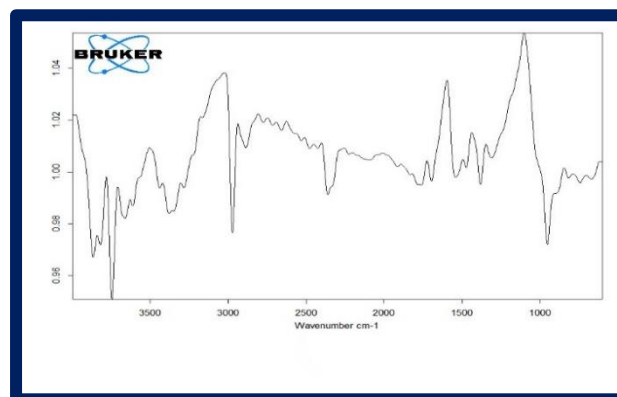
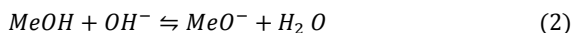




Figure (8): FTIR-Spectrum

5.3. Chemical composition

XRF was applied for determining the structural formula related to prepared samples. XRF analyses have indicated that Natural Zeolites has been majorly composed of Al<sub>2</sub>O<sub>3</sub> (11.437%) and SiO<sub>2</sub> (45.104 %) succeeded by Fe<sub>2</sub>O<sub>3</sub> (8.449%), CaO (7.276%), MgO (4.183%), Na<sub>2</sub>O (2.432%), K<sub>2</sub>O (2.18%), TiO<sub>2</sub>(1.257%), MnO(0.086%), and P<sub>2</sub>O<sub>5</sub>(0.851%). In existence of aqueous solutions, surface OH groups were developed on such oxide types. Results have exhibited that 0.270mmol/g surface OH groups have been present on PMN550 catalyst surface. OH groups that have been formed on the surfaces of the metal oxide have played the role of Brnsted acid sites



In which, Me OH<sub>2</sub><sup>+</sup>, Me OH, and MeO<sup>-</sup> are representing the protonated, neutral, and de-protonated surface OH groups.

5.4. X-ray diffraction (XRD)

XRD has been defined as the major analytical method that is.

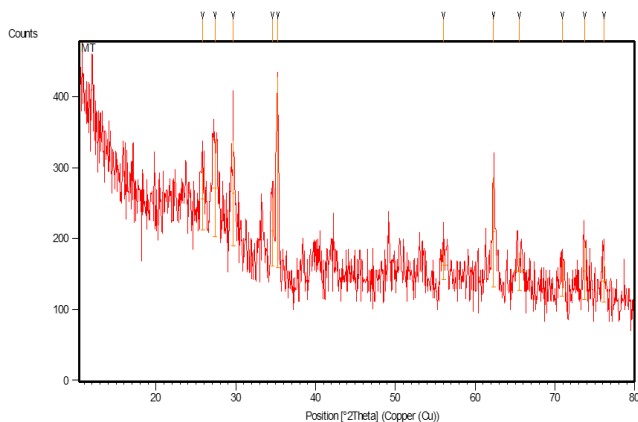


Figure (9): XRD Diagram

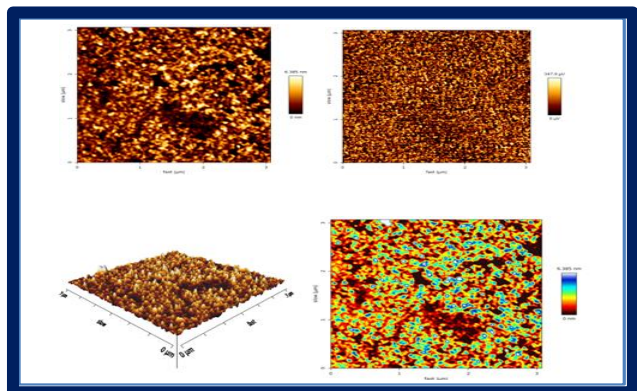


Figure ( 10): AFM particle size distribution with average diameter

used to determine the grain size, phase composition, and crystal structures of materials. Based on pigments’ distribution, the material composition might be analyzed (qualitatively) through comparing the powder diffraction. In addition, the catalysts’ XRD analysis was conducted at the temperature of the room within a range of Bragg angle 10° ≤ 2θ ≤ 90° at 2°min<sup>-1</sup> scanning speed via X-ray diffract meter, with the use of Cu K α- radiation (λ=3.44690 Å°). The results indicates that the main PMN550 sample phases have been anorthite, albite, and hematite. PMN550 catalyst exhibited many patterns of XRD.

5.5. Pore volume and Surface area analyses

The pore volume and surface area have been measured for prepared PMN550. Table 2 shows the pore volume, surface area, and pore sizes of synthesized PMN550. It may as well be observed that after calcination, surface area and pore volume have been slightly decreased because of the occupation regarding active component in certain spaces within samples. The micrographs showed that the particles of the catalyst had higher agglomeration, while individual granules corroded and rough surfaces that which might be because of particles’ attrition throughout reaction and the reacting materials’ settling on the surface of the catalyst.

Table(2): Summary of pore volume, surface area, and pore size of PMN550 catalyst

Catalyst	Surface area (m <sup>2</sup> /gm)	Pore size (nm)	Pore volume (cm <sup>3</sup> /gm)
PMN550	0.4703	12.71315	0.001495

6. (CODS) of heavy naphtha

The effect of the operational parameters on the efficiency of the catalytic process and desulfurization was studied. Through reactor type a batch reactor, it was investigated to increase the effect of the ratio of H<sub>2</sub>O<sub>2</sub>/HN (from) 0.1-0.6(. The results showed that the efficiency of desulfurization of HN increased when the ratio was increased. As all other variables were constant at the optimum values (PH = 1, weight of the catalyst = 0.01 g, temperature = 80 °C and time=60min). The maximum value was reached at 0.4 It was noted that increasing the volume ratio to more than 0.4 leads to a sharp decrease in the efficiency of desulfurization of HN in the presence of PMN550 and a direct increase in the efficiency of removing sulfur from HN by increasing the ratio from (0.1-0.4) specifically, and this efficiency was from (60%-65%), respectively as shown in Fig. 11 The ratio of (H<sub>2</sub>O<sub>2</sub>/HN) produces the hydroxyl ion (OH<sup>-</sup>) and the performance acid CH<sub>2</sub>O<sub>3</sub>, and the increase of these two leads to an increase in the oxidation efficiency of organic sulphur compounds to form a sulfate radical and adsorption over the PMN550 catalyst, decomposing hydrogen peroxide to the hydroxyl group (OH<sup>-</sup>) and a highly reactive hydroxyl radical (OH<sup>•</sup>) equation (3). Sulfur compounds are attacked by the hydroxyl radical according to Equation (4) Haw et al. [14].Haw et al. reported that hydrogen peroxide decomposes to water and gaseous oxygen, (Equation (5)), it competes with the previous pathway that forms hydroxyl radicals Melada et al. [15]. Inhibition of the formation of hydroxyl radicals leads to inhibition Desulfurization process.

This leads to poor performance of PMN550 beyond ratio (0.4) Unlike PMN550, which is rich in oxygen molecules, which acts as a stabilizer for H<sub>2</sub>O<sub>2</sub> and prevents its decomposition to H<sub>2</sub>O, O<sub>2</sub> [15]. It is not confirmed completely the role of diffusion in decreasing the desulfurization activity above the ratio of H<sub>2</sub>O<sub>2</sub> to HN of 40%.

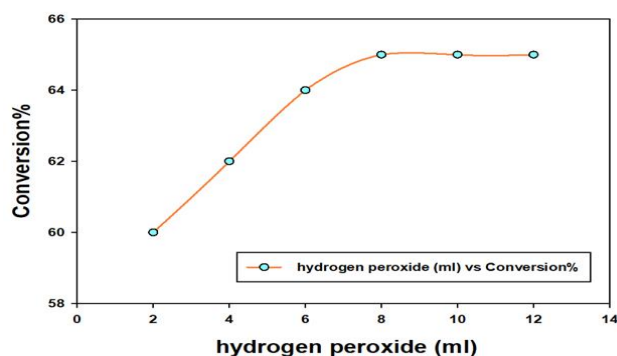
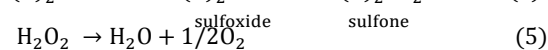
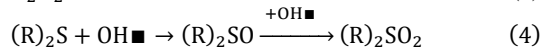
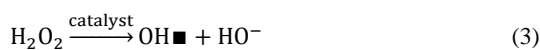


**Figure (11):** Effects of the hydrogen H<sub>2</sub>O<sub>2</sub> to the ratio of the heavy naphtha (H<sub>2</sub>O<sub>2</sub>/HN) on efficiency of percentage de-sulfurization at optimal conditions.

**Fig. 12** shows that increasing the dose of formic acid to heavy naphtha (H<sub>2</sub>O<sub>2</sub>/HN) leads to a decrease in the desulfurization process at a rate higher than 15%, while the initial optimum conditions are, (CH<sub>2</sub>O<sub>2</sub>/HN = 0.15, catalyst weight = 0.01 g, temperature = 80 °C, time = 60 minutes). Due to the low acidity of the solution PH and, as a consequence, the efficiency of the catalytic oxidation process for desulfurization was negatively affected. Formic acid reacts with hydrogen peroxide to produce performic acid (CH<sub>2</sub>O<sub>3</sub>), which has a major role in the catalytic oxidation process of desulfurization Yu et al. [16]. The efficiency of the catalytic oxidation process of removing sulfur decreases if the dose of formic acid is more than 3 ml and this is due to three things [16]. The first is that the thermal adsorption of organosulfur compounds on the surface of PMN550 decreases, and their ability to collide with the active sites of oxygen also decreases.

Second, it is possible to push free radicals from hydroxyl OH<sup>•</sup> generated from H<sub>2</sub>O<sub>2</sub> on the surface of carbon. Finally, PMN550 has strong affinity

with HN, and can be easily fractionated. PMN550 acts as a phase transfer agent between the formed performance acid and refractory organosulfur compounds as a very effective pathway in the catalytic oxidation process for the removal of refractory organosulfur compounds.

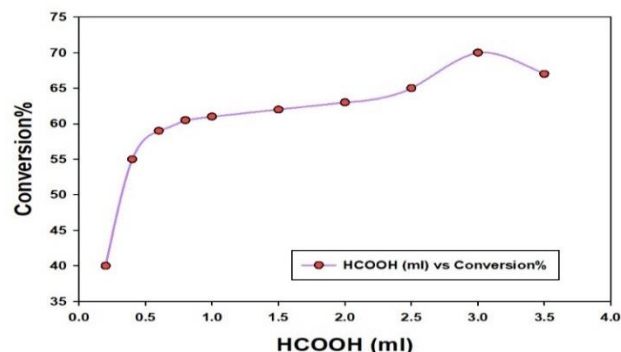


**Figure ( 12 ):** Effects of the pH of the solution on the efficiency of the percentage de-sulfurization at the optimal conditions.

**Fig.13.** Increasing of PMN550 catalyst under optimal conditions. (H<sub>2</sub>O<sub>2</sub>/HN=0.4, CH<sub>2</sub>O<sub>3</sub>=0.15, PH=1, T=80Co, time=60min). leads to an increasing of the surface area, thus increasing the efficiency of the catalytic oxidation process to remove organic sulfur compounds (CODS).

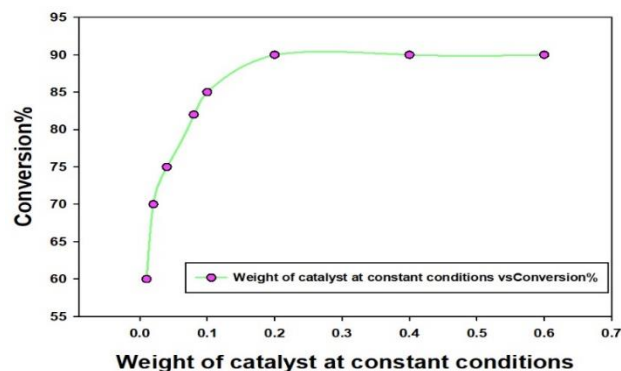


**Figure (13):** Effects of the catalyst weight upon the efficiency of the percentage de-sulfurization at the optimal conditions.

Increasing the temperature from (12-20) °C at the optimal conditions for the rest of the variables. (H<sub>2</sub>O<sub>2</sub>/HN) =0.4, (CH<sub>2</sub>O<sub>2</sub>/HN) =0.15, PH=1 and time=60min. increasing the efficiency of the catalytic oxidation process to remove the organic sulfur compounds from the heavy naphtha product. As shown in **Fig. 14** This is due to the production of large quantities of active oxygen and the oxidation of the organic sulfur compounds at high temperatures. This is to accelerate the reaction with these compounds when the temperature rises from (20-90) °C. Also, increasing the temperature reduces the viscosity of the solution [17]. Thus, it facilitates the penetration of the solution into the pores of the catalyst PMN550, and

thus spreads on the outer and inner surfaces (external and internal diffusion) inside the pores of the catalyst Zeolite (PMN550).

Thus, it enhances the efficiency of the catalytic oxidative process of the reaction of organic sulfur compounds. Forming sulfonates and sulfoxides that are separated, by the extraction process. Increasing the temperature to above (90°C) did not result in any increase in the efficiency of the process, making (90 °C ) the best thermal temperature in economic terms. Raising the temperature above (90 °C ) Useless.

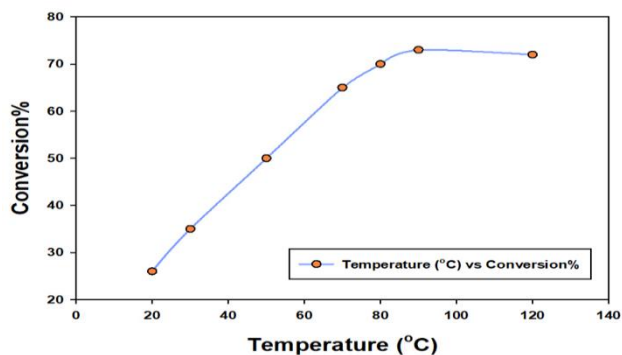


**Figure (14): Effects of the temperature on the efficiency of the percentage desulfurization at the optimal conditions.**

The residence time inside the reactor mainly affects the efficiency of the catalytic oxidation process of sulfur desulfurization through the decomposition of organic sulfur compounds in the optimal conditions for the process. ( $H_2O_2/HN$ ) =0.4, ( $CH_2O_2/HN$ ) =0.15, PH=1, T=90°C and time=60min as noted in **Fig. 15**. In addition, increasing the residence time increases the adsorption of organic sulfur compounds on the surface of the catalyst and between the internal pores, for PMN550, which increases the adsorption efficiency Srivastava et al. [18]. No change in the efficiency of the process was observed when the residence time was increased to more than 60 minutes. The reason is due to the presence of a semi-equilibrium state. Perhaps the presence of many vacant active sites on the surface and inside the catalyst in the first 60 minutes. After that, no more adsorption occurred due to the saturation of these sites [18]. Regeneration of catalysts must be carried out in order for these catalysts are reused again after being saturated with organic sulfur compounds. In the present work, reactivation of PMN550 is inexpensive although PMN550 catalyst was used, more than once after its use in the process of oxidation and saturation with sulfur compounds and without reactivation and gave high results.

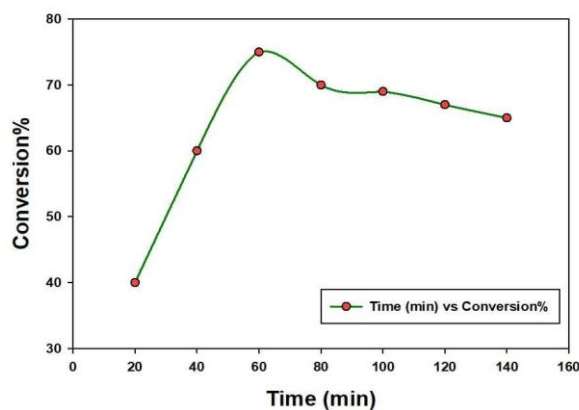


**Figure (15): Effects of the time of the contact on the efficiency of the percentage de-sulfurization at optimal conditions.**

### 6.1. Effect of types of organic acid on the Oxidative desulphurization of heavy naphtha

In **Fig. 16**, the effect of different acids on the catalytic oxidation process was studied in the presence of hydrogen peroxide to react with it to form performance acid. The maximum removal process was with sulfuric and formic acids at the beginning of the tests, where the removal rates were 50% and 55%, respectively. Whereas, other acids such as glacial acetic acid, malic acid and acid phthalates. The percentage of organic sulfur compounds removed was 47%, 45% and 40%, respectively. Previous research indicated that these oxidants have a high selectivity for the oxidation of organic sulfur compounds. [17-19]. Sulfur compounds that predominate mainly thiophene, alkylthiophene and benzo Thiophene (BZT) Song et al. [20] Low molecular weight thiophenes are easily oxidized by these oxidants compared to complex polycyclic thiophenes Ali et al. [19].

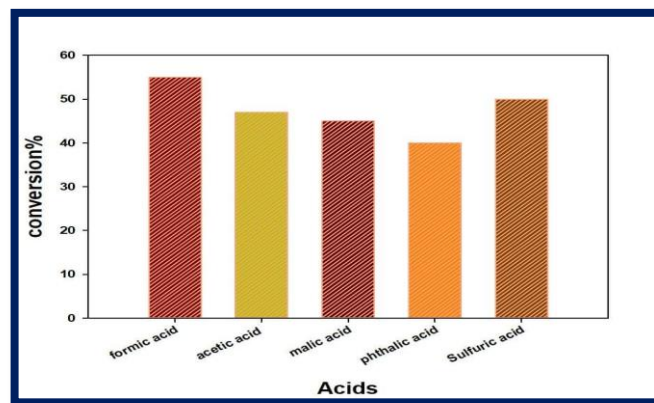


**Figure (16): % Desulphurization of heavy naphtha with organic oxidants.**

Oxidation mechanism of formic acid with hydrogen peroxide and the presence of a donated proton. Formic acid is a strong acid. non-selective oxidation undergone by phthalic acid. It oxidizes other functional groups, other than sulfur moieties, such as hydrocarbons, elevated olefins. Its formation associated with resonance-stable benzoate ions is the reason for this. Malic acid also has to be very weak because the anion (maleate ion)

formed is stabilized by the double bond and the carbonyl effect of the groups ... Thus, instead of being used by oxidation, the formed anion will react with a proton to form an acid.

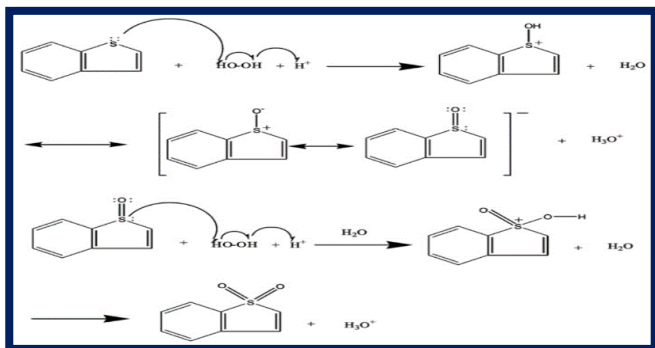


**Figure (17): Oxidation mechanism with H<sub>2</sub>O<sub>2</sub> in presence of a proton.**

As a result, in the order sulfides, disulfides > benzothiophenes > thiophenes, the reactivities of oxidation of organosulfur compounds have been decreased. The oxidation reactivities related to thiophenes and benzothiophenes were increased by methyl substituents, most likely because of the increase in the electron density on atom of sulfur Otsuki et al. [23]. Sulfuric acid catalyzed oxidation with H<sub>2</sub>O<sub>2</sub> Yazul et al. [22]. showed a similar reactivity trend [19]. The organosulfur components have been smoothly oxidized with H<sub>2</sub>O<sub>2</sub> with the existence of HCOOH in this work, resulting in the formation of peracetic acid. As a result, oxidative treatment will be beneficial for naphtha's ODS. HDS also serves as an effective pretreatment for ODS by removing thiophenes that are resistant to oxidations, which is why, the sequential ODS and HDS treatments for the ultra-deep de-sulfurization of heavy naphtha should be effective.

### 6.2. Effect of Extraction on the Oxidized Model Oil (Heavy Naphtha)

The polar solvents were utilized in order to extract oxidized oil, in the process of the ODS. In this research, the solution of the methanol water (80: 20) has been utilized to extract the model oil that has been oxidized in presence of the PMN 550. For the purpose of investigating the solution of methanol water (80: 20) extraction efficiency, extracted sulfur compounds' concentration has been researched. The sulfur concentration balance in the extract of the heavy naphtha, following catalytic oxidation, has been illustrated in **Fig. 18**. data has revealed that the model S compounds might be extracted slightly by solution of the methanol water with the oxidization of heavy naphtha. On the other hand, in the cases of the catalytic oxidation that is followed by heavy naphtha extraction, about 90% of S has been eliminated. Throughout the step of the extraction, all compounds of oxidized sulfur have been shifted to the solution of the methanol water. The results that have been listed in **Table 3** have shown that the desulfurization yield of 1st, 2nd, 3rd and 4rd extraction stage was 90, 92, 95 and 99%. It has been observed from results that following the 2nd extraction did not show sever changes in the efficiency of the de-

sulfurization, which suggests that the extractions in 4 stages have been helpful in the maximal oxidized sulfur compounds' removal. Due to the high solvent system polarity, the heavy naphtha recovery yield has been very good, approximately 98% - 99%, the minor yield loss could be resulting from the handling throughout the process of the extraction.

**Table 3. desulfurization Extraction cycles.**

Extraction cycles	Conversion %	Sulfur content (ppm)
1	90	64.83
2	92	51.804
3	95	32.265
4	99	8.07

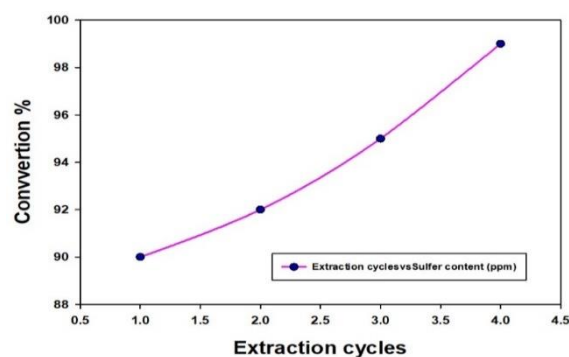


**Figure (18): Desulfurization of heavy naphtha in presence of the PMN550 catalyst with several extractions with the methanol-water**

## 7. Sulfur adsorption kinetic study

Sulfur adsorption kinetics on the PMN550 have been investigated in order to determine best-fitting order of the adsorption. The correlation coefficient ( $R^2$ ) have been used to compare the experimental data to the predicted model, and the ( $R^2$ ) value closest to unit has indicated the correct model for adequately describing kinetics. In addition, the  $\ln(q_e - qt)$  curve as a time function  $t$  **Fig. 19**. The kinetic equation was used for The Lagergren's pseudo first order [24].

$$\log(q_e - q_t) = \log(q_e) - k_1 \frac{t}{2.303} \quad (2)$$

**Table 4. Experimental data**

Wight of catalyst (gm)	0.2
Amount heavy naphtha feed stock ( ml)	20
Amount hydrogen peroxide (ml)	8
Amount formic acid (ml)	3
Temperature °C	90
Time contact (mint)	60
Sulfur content (ppm)	64.83
Conversion%	90
Amount if adsorption (mg/g)	0.009090285



**Table 5. Kinetic calculation of pseudo first order**

intercept	0.003850579
slope	-1.47822E-05
qe Experimental(mg/gm)	0.009090285
qe Theroretical(mg/gm)	1.008905707
K1	3.40434E-05
R2	0.3104

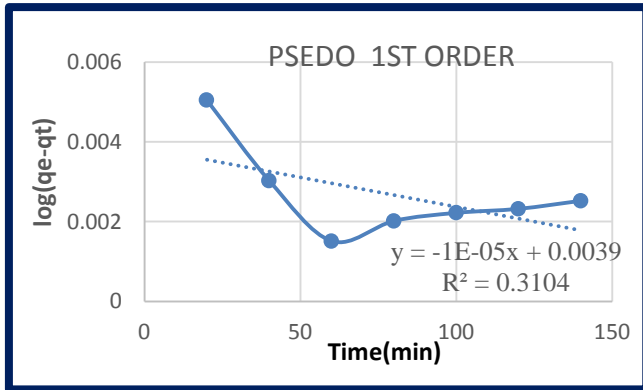


**Figure (19): Time versus log (qe-qt) pseudo 1st order kinetic**

In this condition, **Fig. 20** provides a linear correlation that allow computing qe from slope and k2 to ordinate to the originally. **Table 6** is used to group the second- order constants. Pseudo second-order kinetic used in calculation Ho et al. [25].

$$\frac{t}{q_t} = \frac{1}{q_e^2 * K_2} + \frac{1}{q_e} * t \tag{3}$$

**Table 6. Pseudo second-order kinetic calculation**

Ce	time(min)	qt	t/qt	Ce
0.039048	20	0.00404271	4947.176523	0.039048
0.026022	40	0.00606174	6598.765371	0.026022
0.0162525	60	0.007576013	7919.733501	0.0162525
0.019509	80	0.007071255	11313.40901	0.019509
0.0208116	100	0.006869352	14557.41386	0.0208116
0.0214629	120	0.006768401	17729.4473	0.0214629
0.0227655	140	0.006566498	21320.3462	0.0227655

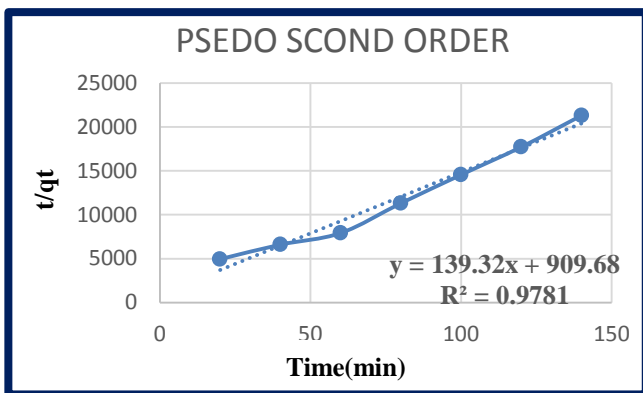


**Figure (20): Pseudo second-order relation**

The benefit of utilizing such model is that there’s no requirement for knowing the equilibrium’ capacity from experiments, as it might be specified from the model via attempting first- and second-order, it can be noted that the second-order showed more accuracy ( $R^2=0.9781$ ) compared to the first-order  $R^2=0.342$ .

**Table 7. Kinetic calculation of pseudo second order**

intercept	909.6769305
slope	139.3188451
qe Experimental(mg/gm)	0.009090285
qe Theroretical(mg/gm)	00717778
K2	5.66361E-08
R²	0.9781

**8. Study of adsorption isotherms**

Isotherms were investigated in order to better understand the adsorption phenomenon, such isotherms were determined using a catalyst, a batch process in naphtha solution of 20 mL, and an initial sulfur concentration of 651.3ppm. The solution has been kept shaken to ensure that sulfur is distributed uniformly over the solution. For specific temperatures of ° C, the sulfur concentration in the solution has been monitored as a time function. Furthermore, the concentration of the equilibrium has been determined, and the amount of the sulfur that has been adsorbed on catalyst has been assessed using the formula:

$$q_e = (C_o - C_e) * v/m \tag{4}$$

where: qe: represents amount of sulfur that is being adsorbed on the equilibrium PMN550 (mg/g),  
 C o: represents the sulfur’s initial concentration in the solution (mg/L),  
 m: represents the catalyst mass(g),  
 C e: represents the sulfur concentration in the solution at the equilibrium (mg/L),  
 V: represents the solution’s volume (L).

**8.1. Freundlich isotherm**

The Freundlich model, which indicates heterogeneity at the adsorbent’s surface, has been used to calculate the adsorption capacity using the next formula:

$$Q_e = K_f * C_e^{\frac{1}{n}} \tag{5}$$

where Q e represents the amount of metal adsorbed per gram of adsorbent at equilibrium (mg/g). K f constant of Freundlich isotherm (mg/g) n represents the adsorption intensity; Ce represents the equilibrium concentration of the adsorbent (mg/L) the Freundlich equation in logarithmic form according to the relationship:

$$\log Q_e = \log K_f + \frac{1}{n} \log C_e \tag{6}$$

The experimental results obtained for isotherms given in **Fig. 21**

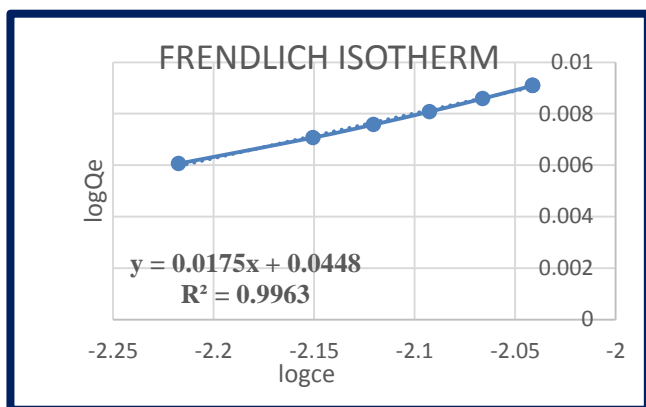


Figure (21): Freundlich isotherm for adsorption at all catalyst loading

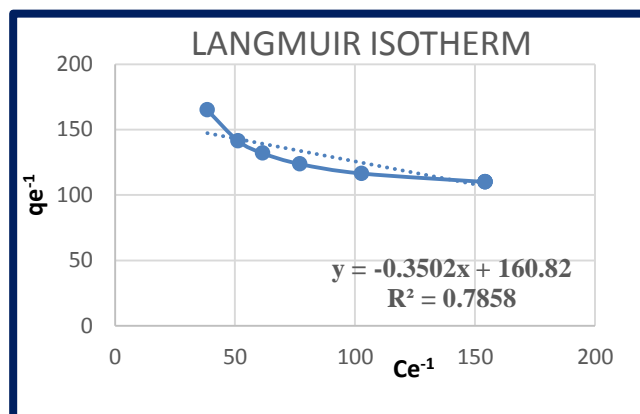


Figure (22): Langmuir's isotherm for the adsorptions at all of the catalyst loadings

Table 8. The experimental results Freundlich isotherm

intercept	-2.598416659
slope	-0.258321367
qe Experimental(mg/gm)	0.009090285
qe Thermostical(mg/gm)	0.007741526
$K_f$	0.002521061
n	-3.871147055
$R^2$	0.9963

The curve showing the isotherms in Fig. 21 indicates that adsorption is following the model of Freundlich, that experimental results could be correlated using Freundlich eq., and that the coefficients of the correlation have been near the unity. The isotherms were used to calculate the Freundlich constants K and n.

### 8.2. Langmuir isotherm

Langmuir model can be used if a monolayer has been adsorbed and if the adsorbed molecules interact. Based on the next relationship, the Langmuir's eq. is applied for just 1 mono-layer that is being adsorbed with well-defined number of the identical and uniform adsorption sites:

$$q_e = \frac{Q_o \cdot K_L \cdot C_e}{(1 + K_L \cdot C_e)} \quad (7)$$

$C_e$  represents the concentration of equilibrium of adsorbate (mg/L),  $q_e$  represents the adsorbed metal amount for each gram of adsorbent at the equilibrium (mg/g).  $Q_o$  represents the maximal capacity of the monolayer coverage (mg/g)  $K_L$  represents the Langmuir isotherm constant (L/mg). Langmuir's eq. might be represented as: Through the representation of experiment results, based on Langmuir's equation gives isotherms of Fig. 22.

Table 9. The experimental results Langmuir isotherm

intercept	160.8222984
slope	-0.350242525
qe Experimental(mg/gm)	0.009090285
qe Thermostical(mg/gm)	0.00747
$K_L$	-459.1741063
RL	-0.034594882
$R^2$	0.7858

$K_L$  represents a constant associated with adsorption energy (Langmuir's model).  $R^2$  value that is not more than unity is representing a favorable, meaning that the model is not favorable as well.

### 8.3. Isotherm of Temkin

$$q_e = \frac{RT}{b} \ln(A_T \cdot C_e) \quad (8)$$

$$q_e = \frac{RT}{b} \ln A_T + \left(\frac{RT}{b}\right) \ln C_e \quad (9)$$

$$B = \frac{RT}{b} \quad (10)$$

$$q_e = B \ln A_T + B \ln C_e \quad (11)$$

This isotherm has been applied as follows [26, 27].

$A_T$  = Temkin isotherm equilibrium binding constant (L/g),  $b$  = Temkin isotherm constant,  $R$  = universal gas constant (8.314 J/mol/K),  $T$  = Temperature K,  $B$  = Constant that is associated with the heat of sorption (J/mol).

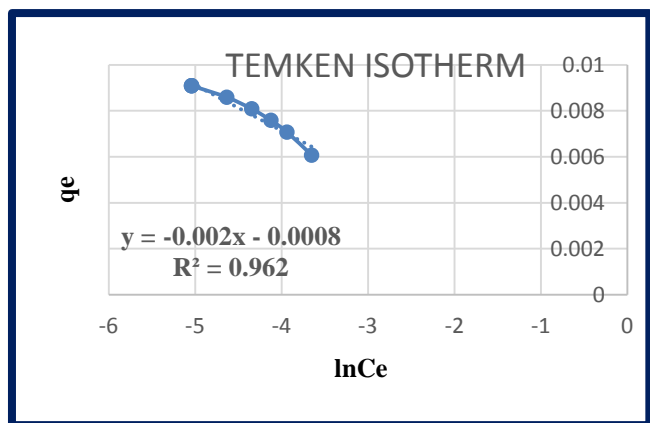


Figure (23): Temkin isotherm for all catalysts type.

Table 10. The experimental results Temkin isotherm

intercept	-8.46861
slope	-19.95247
qe Experimental(mg/gm)	0.009090285
qe Thermostical(mg/gm)	0.007618723
AT	1.528732891
b	-1512585.811
R <sup>2</sup>	0.962

The qe curve vs. Ln Ce Fig. 23 provides the ability for determining isothermal A & B constants from interception and slope. Experimental results may be correlated by Temkin eq. and the coefficients of the correlation are near unity, meaning that the model can represent practical data, but it is not the best of them for those catalyst PMN 550 types. Temkin constant values A T & b have been determined from isotherms .

Table 11. The summary of the results of the isotherm .

Isotherm	parameters	PMN550
Freundlich	qe(mg/gm)	0.007741526
	K <sub>f</sub>	0.002521061
	n	-3.871147055
	R <sup>2</sup>	0.9963
Langmuir	qe(mg/gm)	0.00747
	K <sub>L</sub>	-459.1741063
	R <sub>L</sub>	-0.034594882
	R <sup>2</sup>	0.7858
Temkin	qe(mg/gm)	0.007618723
	AT	1.528732891

b	-1512585.811
R <sup>2</sup>	0.962

Table 12. the optimum condition in experimental

variable	unit	value	conversion
Weight of catalyst	gm	0.2	99%
temperature	k	363	
time	min	60	
Hydrogen peroxide	ml	8	
Formic acid	ml	3	
Number extraction cycle	-	4	

### 9. Conclusions

The catalytic oxidation of organic sulfur compounds using CH<sub>2</sub>O<sub>2</sub> and H<sub>2</sub>O<sub>2</sub> together with the PMN550 catalyst showed a high efficiency to remove the organic sulfur compounds from HN up to 99%. The initial sulfur content of a real sample of heavy naphtha ore produced in Iraqi refineries / Doura refinery = 651.3PPM at optimum operating conditions. Increasing the ratio (H<sub>2</sub>O<sub>2</sub>/HN, CHO<sub>2</sub>O<sub>2</sub>/HN) promotes an increase in the efficiency of the process of removing organic sulfur compounds from HN to reach the maximum percentage of 40% and 15%, respectively, due to the formation of hydroxyl ions (OH<sup>-</sup>) and the formation of (CH<sub>2</sub>O<sub>3</sub>) performance acid, which led to the cracking of (HN) through the formation of) SO<sub>4</sub>--2 (which was adsorbed by PMN550 catalyst. PMN550 catalyst showed stability in oxidative activity after 40% enrichment of oxygen molecules, which prevents the decomposition of (H<sub>2</sub>O<sub>2</sub>) to (O<sup>-</sup>) and( H<sub>2</sub>O). The increase in (PH) resulting from formic acid is favorable for the oxidation of organic sulfur compounds. Formic acid and hydrogen peroxide react to produce a performance acid (para-acid CH<sub>2</sub>O<sub>3</sub>) which accelerates the catalytic oxidation process of organic sulfur compounds. The low pH value is a suitable environment for the reaction and formation of CH<sub>2</sub>O<sub>3</sub> acid. The surface area of PMN550 and its active sites increases with increasing amount of catalyst (a positive relationship) and this enhances the efficiency of the catalytic oxidation process (CODS) of organic sulfur and desulfurization compounds. Temperature is important in the catalytic oxidation process, **where it** removes organic sulfur compounds (CODS) .Increasing the temperature to (90 °C ) increases the production of active oxygen, which accelerates the oxidation reaction of organic sulfur compounds, reduces the viscosity of the solution and thus allows penetration and movement within the narrow catalytic pores to be reacted on the outer and inner surfaces within the channels. and catalytic ducts, especially for heavy fluids. Increasing the residence time to 60 minutes increases the efficiency of the CODS process for liquid reactants by increasing the ratio of oxygen to organic sulfur compounds. Increasing the residence time to 60 minutes increases the contact between the PMN550 catalyst and the organic sulfur compounds, which enhances the efficiency of the adsorption process. The optimization technique to find the optimal (CODS) process kinetic parameters with the use of 2 approaches (i.e. the **linear** and the **nonlinear**) based on experimental results can be used with higher degree of the confidence. It has been noticed that the 2nd approach (i.e. the non-

linear) has shown a higher degree of the accuracy according to minimization of Summation of Square Error (SSE) between the experimental and the expected results with the MAE of <5% between all results at different operation conditions.

The mathematical model obtained can be utilized to find the optimal operating conditions for improving the fuel quality for the purpose of obtaining free sulfur content.

## REFERENCES

- H.J. Chang, G.L. Cho, Y.D. Kim, The economic impact of strengthening fuel quality regulation-reducing sulfur content in diesel fuel, *Energy Policy* 34 (2006) 2572–2585.
- J. Eber, P. Wasserscheid, A. Jess, Deep desulphurization of oil refinery streams by extraction with ionic liquids, *Green Chem.* 6 (2004) 316–322.
- R.T. Yang, *Adsorbents: Fundamentals and Applications*, Wiley, New York, 2003.
- G. Murali Dhar, G. Muthu Kumaran, M. Kumar, K.S. Rawat, L.D. Sharma, B. David Raju, K.S. Rama Rao, Physico-chemical characterization and catalysis on SBA-15 supported molybdenum hydrotreating catalysts, *Catal. Today* 99 (2005) 309–314.
- S. Dasgupta, V. Agnihotri, P. Gupta, A. Nanoti, M.O. Garg, A.N. Goswami, Simulation of a fixed bed adsorber for thiophene removal, *Catal. Today* 141 (2009) 84–88.
- M. Ishaq, M. Shakirullah, I. Ahmad, M. Khan, Removal of mercaptan sulfur from some petroleum fractions with tiobacillus thiooxidans, *Chem. Indian J.* 2 (2005) 68–74.
- I. Bagus, W. Gunam, Y. Yaku, M. Hirano, K. Yamamura, F. Tomita, T. Sone, K. Asano, Biodesulfurization of alkylated forms of dibenzothiophene and benzo(b)thiophene by *Sphingomonas subarctica* T7b, *J. Biosci. Bioeng* 101 (2006) 322–327.
- H. Li, L. He, J. Lu, W. Zhu, X. Jiang, Y. Wang, Y. Yan, Deep oxidative desulfurization of fuels catalyzed by phosphotungstic acid in ionic liquids at room temperature, *Energy Fuels* 23 (2009) 1354–1357.
- W. Wang, S. Wang, H. Liu, Z. Wang, Desulfurization of gasoline by a new method of electrochemical catalytic oxidation, *Fuel* 86 (2007) 2747–2753.
- W. Trakarnpruk, K. Rujiraworawut, Oxidative desulfurization of gas oil by polyoxometalates catalysts, *Fuel Proc. Technol.* 90 (2009) 411–414.
- Krehula, S.; Musić, S. The influence of Cd-dopant on the properties of  $\alpha$ -FeOOH and  $\alpha$ -Fe<sub>2</sub>O<sub>3</sub> particles precipitated in highly alkaline media. *J. Alloy. Compd.* 2007, 431, 56–64.
- J. W. Ward, "Infrared studies of zeolite surfaces and surface reactions," in *Zeolite Chemistry and Catalysis*, J. A. Rabo, Ed., ACS Monograph no. 171, pp. 118–284, American Chemical Society, Washington, DC, USA, 1976.
- E. M. Flanigen, H. Khatami, and H. A. Szymanski, "Infrared structural studies of zeolite frameworks," in *Molecular Sieve Zeolites-I*, E. M. Flanigen and L. B. Sand, Eds., *Advances in Chemistry Series* 101, pp. 201–210, American Chemical Society, Washington, DC, USA, 1971.
- Haw, K.-G., Bakar, W. A. W. A., Ali, R., Chong, J.-F. and Kadir, A.A.A., "Catalytic Oxidative Desulfurization of Diesel Utilizing Hydrogen Peroxide and Functionalized-activated Carbon in a Biphasic Diesel-acetonitrile System," *Fuel Processing Technology*, 91, 1105-1112(2010).
- Melada, S., Pinna, F., Strukul, G., Perathoner, S., Centi, G., "Direct Synthesis of H<sub>2</sub>O<sub>2</sub> on Monometallic and Bimetallic Catalytic Membranes Using Methanol as Reaction Medium," *J. Catalysis*, 237, 213-219(2006).
- Yu, G. X., Lu, S. X., Chen, H. and Zhu, Z. N., "Diesel Fuel Desulfurization with Hydrogen Peroxide Promoted by Formic Acid and Catalyzed by Activated Carbon," *Carbon*, 43, 2285-2294(2005).
- Zadyмова, N. M., Skvortsova, Z. N., Traskine, V. Y., Kulikov-Kostyushko, F. A., Kulichikhin, V. G. and Malkin, A. Y., "Rheological Properties of Heavy Oil Emulsions with Different Morphologies," *J. Petroleum Science and Engineering* 149, 522-530(2017).
- Srivastav, A. and Srivastava, V. C., "Adsorptive Desulfurization by Activated Alumina," *J. Hazardous Materials*, 170, 1133-1140 (2009).
- M.F. Ali, A. Al-Malkib, S. Ahmed, Chemical desulphurization of petroleum fractions for ultra-low sulfur fuels, *Fuel Process. Technol.* 90 (2009) 536–544.
- Song, C., Ma, X., (2006), Ultra-clean diesel fuels by deep desulfurization and deep dearomatization of middle distillates, in: *Practical Advances in Petroleum Processing*, Springer, New York.
- S. Otsuki, T. Nonaka, N. Takashima, W. Qian, A. Ishihara, T. Imai, T. Kabe, Oxidative desulphurization
- K. Yazul, S. Sato, Y. Sugimoto, A. Matsumura, I. Saito, Tungstophosphoric acid catalyzed oxidative desulphurization of naphtha with hydrogen peroxide in naphtha/acetic acid biphasic system, *J. Jpn. Pet. Inst.* 50 (2007) 329–334.
- Otsuki, S., Nonaka, T., Takashima, N., Qian, W., Ishihara, A., Imai, T., Kabe, T., *Energy & Fuels*, 14, 1232 (2000).
- Zafar, S., Khalid, N., Daud, M., & Mirza, M. L. (2015). Kinetic studies of the adsorption of thorium ions onto rice husk from aqueous media: linear and nonlinear approach. *The Nucleus*, 52(1), 14-19.
- Ho, Y. S., & McKay, G. (1999). Pseudo-second order model for sorption processes. *Process biochemistry*, 34(5), 451-465.
- Kozlovsky, Y., Chernomordik, L. V., & Kozlov, M. M. (2002). Lipid intermediates in membrane fusion: formation, structure, and decay of hemifusion diaphragm. *Biophysical journal*, 83(5), 2634-2651.
- Roundhill, D. M., & Koch, H. F. (2002). Methods and techniques for the selective extraction and recovery of oxoanions. *Chemical Society Reviews*, 31(1), 60-67.